AIAA JOURNAL
Vol. 45, No. 1, January 2007

Structural Damage Localization Using Element Signature Recognition

Frank P. Lopez* and David C. Zimmerman†
University of Houston, Houston, Texas 77023

DOI: 10.2514/1.19796

In damage detection algorithms the use of mode-force error arising from reduced analytical system matrices precludes the possibility of stiffness damage localization for those elements residing entirely outside the analysis set. Subsequently, any indication of mode-force error arising from damage appears as a force imbalance in each reduced degree of freedom due to the erroneous load paths introduced in the reduction process. The result is a smearing of the otherwise localized nature of the error thereby altering the interpretation of perturbation matrix-based damage detection results. To address this issue this work seeks to reconcile the inherent dimensional mismatch between finite element models and incomplete measured modal data by use of a subspace recognition procedure based on the problem of subset selection. The spatial characteristics of the reduced dynamic residual are assumed to represent a characteristic signature of a damaged element or set of elements where a signature is defined as the significant vector basis spanning the reduced residual matrix as defined by a singular value decomposition process. Stiffness damage is thereby localized by a measure of the subspace intersection dimension of the experimentally measured signature with analytically regenerated candidate elemental signatures. The analytically regenerated signatures arise from a mapping of elemental stiffness matrix sets via the transformation procedure used in the reduction process and the measured modal matrix. Multiple signatures are identified after an orthogonalization of the original target signature with respect to the most consistent signature in the previous iteration. For damage localization to be possible each mapping must project a nonnull and unique signature in the analysis set residual. This work is evaluated on damage simulations of a 155 mm aeroshell and the NASA Langley Research Center eight-bay experimental test bed.

Nomenclature

B	=	dynamic residual matrix
f	=	vector of external forces
H	=	an arbitrary square matrix
$I(r)$	=	summation of percent normalized singular values
K	=	FEM stiffness matrix
K_e^j	=	jth elemental stiffness matrix
k	=	index
M	=	FEM mass matrix
n	=	number of global degrees of freedom
p	=	number of analysis-set degrees of freedom
Q	=	orthonormal rotation matrix
r	=	index
T	=	transformation matrix
U	=	matrix of left singular vectors
U_{tar}	=	target signature
U_e^j	=	jth elemental signature
V	=	matrix of right singular vectors
ΔK	=	minimum-rank stiffness perturbation matrix
θ	=	principal angle
Λ	=	diagonal matrix of modal frequencies
Σ	=	diagonal matrix of singular values
Φ	=	modal matrix
$[\,]_d$	=	damaged modal parameter
$[\,]_h$	=	healthy modal parameter
$[\,]_r$	=	reduced system matrix
$\ddot{\cdot}$	=	double differentiation
$\propto$	=	tolerance for transformation matrix null space test

Received 31 August 2005; revision received 14 July 2006; accepted for publication 19 July 2006. Copyright © 2006 by the American Institute of Aeronautics and Astronautics, Inc. All rights reserved. Copies of this paper may be made for personal or internal use, on condition that the copier pay the $10.00 per-copy fee to the Copyright Clearance Center, Inc., 222 Rosewood Drive, Danvers, MA 01923; include the code $10.00 in correspondence with the CCC.

*Research Assistant, Department of Mechanical Engineering, N207 Engineering Building 1, Houston, TX 77204-4006.

†Professor, Department of Mechanical Engineering, N207 Engineering Building 1, Houston, TX 77204-4006.

I. Introduction

THE need for highly accurate analytical models of flexible structures and machinery is required to accurately predict dynamic performance in lieu of costly experimental evaluation. Owing to the complexity of these structures, a common modeling technique is to use the finite element method (FEM). However, it is often the case that due to design parameter misalignment or more commonly physics-based under representation, the physical structure rarely matches the dynamic characteristics of the finite element model. Recent efforts to address this problem have resulted in the development and evaluation of algorithmic methods for structural model refinement. These same algorithms have also demonstrated capability in approaching the damage localization problem. Algorithms used to address FEM refinement can be broadly classified as falling into one of four different approaches: optimal-matrix updates, sensitivity methods, eigenstructure assignment techniques, and minimum-rank perturbation methods. Survey papers providing an overview of these techniques are provided in [1,2]. In the optimal-matrix update formulation, perturbation matrices for the mass, stiffness, and/or damping matrices are determined which minimize a given cost function subject to various constraints. A typical cost function used is the Frobenius norm of the perturbation matrix [3]. Typical constraints may include satisfaction of the eigenproblem for all measured modes, definiteness of the updated property matrices, and preservation of the original sparsity pattern. Sensitivity methods for model refinement and damage localization make use of sensitivity derivatives of modal parameters with respect to physical design variables [4] or with respect to matrix element variables [5]. When varying physical parameters, the updated model is consistent within the original FE program framework, thereby preserving the original load path. Control-based eigenstructure assignment techniques determine the pseudocontrol that would be required to produce the measured modal properties with the initial structural model [6,7]. The pseudocontrol is then translated into matrix adjustments applied to the initial FEM. Finally, the development of a minimum-rank update theory has been proposed as a computationally attractive approach for model refinement and damage detection [8]. The update to each property matrix is of

minimum rank and is equal or less than the number of experimentally measured modes that the modified model is to match.

An outstanding issue in damage assessment procedures is the problem of incomplete modal measurement that arises from vibration measurement testing. The incomplete modal measurement problem is manifested in two forms, experimental measurement of a lesser number of modes of vibration than that of the FEM, and modal test measurements at a subset of the FEM degrees of freedom. Approaches to practically address the latter problem are to either reduce the analytical model to the analysis set of degrees of freedom or to expand the measured modal data to the global set of degrees of freedom [9]. An observed problem with model reduction is that reduction introduces additional nonphysical load paths resulting in smeared residual vectors. An observed problem with mode shape expansion is that errors introduced in the expansion process may become significantly large and lead to a false indication of damage. In this work, a procedure is proposed in which it is assumed the characteristic vector basis of the residual in the analysis-set coordinates is the distinct signature of perturbed elemental matrix sets arising from localized damage [9–11]. The approach identifies perturbed elemental matrix sets by regenerating candidate elemental signatures of a FEM and rating the consistency with the experimentally measured signature in the reduced coordinates.

II. Damage Localization Using Subspace Recognition

The general methodology of the subspace recognition approach is now described.

Step 1: Reduction of the original model to test degrees of freedom. In this step, the original FEM mass and stiffness matrices are dimensionally reduced to the test set of degrees of freedom, resulting in a test analysis model (TAM). Damping is ignored in this case. In this study, Guyan, improved reduced system (IRS), and dynamic reduction are considered. For dynamic reduction, a transformation matrix is generated for each mode of interest. The results of the reduction process are the reduced mass and stiffness matrices, K_r and M_r, and the transformation matrix T.

$$T^T M T = M_r \tag{1}$$

$$T^T K T = K_r \tag{2}$$

This results in system matrices approximating the modal response of the full dimension model but destroys the original load paths created during the FE matrix assembly process.

Step 2: Updating the reduced model using the minimum-rank perturbation theory. The initial modeling error associated with the initial modeling error and that introduced by reduction is removed by updating using the healthy modal measurements. The result is an updated reduced model with an eigensolution consistent with the measured eigendata of the structure in the healthy state. The minimum-rank perturbation theory (MRPT) can be formulated to update multiple property matrices simultaneously. The formulation presented here will assume that the nominal modeling error is entirely located in the stiffness properties of the structure. The formulation of the MRPT for updating the stiffness matrix follows. Suppose that a FEM exists of a structure and is given by

$$M\ddot{\underline{x}}(t) + K\underline{x}(t) = \underline{f}(t) \tag{3}$$

The experimental mode shapes and natural frequencies of the healthy structure are used to formulate the eigenvalue problem which is written as

$$M\Phi_h\Lambda_h + K\Phi_h = \Delta K\Phi_h = B \tag{4}$$

The columns of the dynamic residual B indicate the error between the model dynamics and the experimental data on a mode-by-mode basis. The stiffness perturbation matrix ΔK can be written in factored form as

$$\Delta K = BHB^T \tag{5}$$

where H is a symmetric, full-rank square matrix. Substituting this factorization into Eq. (4) yields

$$BHB^T\Phi_h = B \tag{6}$$

Equation (6) is true if and only if $HB^T\Phi_h = I$, where I is the identity matrix. The matrix H is uniquely calculated as

$$H = (B^T\Phi_h)^{-1} \tag{7}$$

Substituting this result into Eq. (5) gives the unique minimum-rank stiffness perturbation matrix as

$$\Delta K = B(B^T\Phi_h)^{-1}B^T \tag{8}$$

This represents the basic MRPT formulation. A more advanced formulation that uses the singular value decomposition (SVD) instead of the matrix inverse is described in [12].

Step 3: Formulation of the target signature space. In this step, the characteristic vector space of the reduced dynamic residual due to damage is extracted using SVD. The reduced dynamic residual is found with

$$M_{rh}\Phi_d\Delta_d + K_{rh}\Phi_d = B_d \tag{9}$$

The SVD can serve as a rank estimator for matrices which are corrupted with measurement noise. It can also be used to extract a set of basis vectors that span the significant subspace of experimental vector sets. This set of basis vectors is the target subspace of the dynamic residual. The SVD of the dynamic residual is written as

$$B_d = U\Sigma V^T \tag{10}$$

where Σ is a matrix with ordered singular values running along the principle diagonal. The left and right singular vectors are contained in U and V and are unitary matrices. The dynamic residual can be regarded as a summation of p rank-one matrices, where p is the number of measured modes. These rank-one matrices are scaled by an associated singular value. The first rank-one matrix represents the closest rank-one fit to the data contained in the residual. The addition of the second rank-one matrix represents the closest rank-two matrix. The marginal increase in the quality of the numeric fit by addition of subsequent rank-one matrices can be sensed by the magnitude of the corresponding singular values. Subsequently, the relative importance of the basis vectors contained in U and V also follow this scheme. The significant basis vectors in the matrix U representing the dynamic residual vector space are found by the following computation of percent normalized singular values:

$$I(r) = \frac{\sum_{i=1}^{r}\sigma_i}{\sum\sigma} \tag{11}$$

$I(r)$ represents the fractional information retained by the summation of the first r rank-one matrices. The number of significant basis vectors is taken as r when $I(r) \geq \xi$, where ξ is a user prescribed tolerance between 0 and 1. The target subspace is the collection of the significant basis vectors and are grouped together in the matrix U_{tar}, where

$$U_{\text{tar}} = [\underline{u}_1\ \underline{u}_2\ \underline{u}_3\ \cdots\ \underline{u}_r] \tag{12}$$

Step 4: Formulation of elemental signatures. An elemental signature is defined as the consistent vector space of the projection of an elemental matrix onto the reduced set of degree of freedom via reduction transformation and postmultiplication by the measured modal matrix. The formulation of the jth elemental signature starts with finding the reduced elemental stiffness matrix of the jth element.

$$K_{re}^j = T^T K_e^j T \tag{13}$$

where $K_e^j = j$th elemental stiffness matrix or the jth grouping of elemental matrix sets. For simplification, the development will proceed with a signature defined on the basis of a single elemental

stiffness matrix. The projection of the elemental stiffness matrix onto the reduced residual is found by performing the SVD operation on the reduced stiffness element and modal matrix product as shown.

$$K_{re}^{j}\Phi_d = U_e \Sigma_e V_e^T \tag{14}$$

The significant basis vectors are grouped together in matrix U_e^j, where

$$U_e^j = [\underline{u}_1 \ \underline{u}_2 \ \underline{u}_3 \ \cdots \ \underline{u}_n] \tag{15}$$

where $n =$ rank of $K_{re}^j V_d$ as determined by Eq. (11). This process extracts the characteristic vector space in the reduced dynamic residual associated with a perturbation of the jth elemental stiffness matrix.

Step 5: Comparing the target vector space with elemental signatures. The task now is to rate the similarity between the target vector space and each elemental signature in the FEM. We can base a range intersection evaluation of the target signature and an elemental signature by observing the cosines of the principal angles between the two subspaces [13]. Thus, for the jth elemental signature in the model, the principal angles are determined from

$$\mathrm{diag}\,[\cos(\theta)] = \mathrm{SVD}(U_{\mathrm{tar}}^T U_e^j) \tag{16}$$

for $j = 1, 2, 3, \ldots$, where j is an index from 1 to the number of candidate elements. The dimension of the range intersection is defined by s in the following sense:

$$1 = \cos(\theta_1) = \cdots = \cos(\theta_s) > \cdots > \cos(\theta_q) \tag{17}$$

where $q=$ number of measured modes. The above statement implies that if $\cos(\theta_s) = 1$ then s vectors in U_e and U_{tar} span an identical space. In other words, the s vectors represent the same space. Therefore, the single value used to rate the similarity between the vector spaces of U_e and U_{tar} is taken as s in Eq. (17). A perfect intersection dimension is not encountered because the vector space of the reduced dynamic residual has a weakly nonlinear dependence on damage magnitude. In this case we are regenerating an elemental signature based on a 100% stiffness loss. Therefore, in the event of a zero intersection dimension, the most likely case, the first term in Eq. (16) indicates the "closeness" of the two most aligned vectors and is hence taken as the scalar measure of space consistency. The original formulation of the subspace intersection dimension presented in [13] requires that QR decompositions be performed on the matrix arguments to extract orthogonal basis vectors before the SVD operation. In our case, this step is not required because the matrix arguments are already an orthogonal basis vector set.

Step 6: Create new target vector space. Now that an elemental signature that best matches the target vector space has been identified in step 5, the next step is to define a new target vector space. The pseudoinverse is used to eliminate the space spanned by the first best signature from the target vector space. The step assures that in the next iteration, the component of the target vector space that has been matched with an elemental signature will not be matched again. The new target vector space is defined as

$$U_{\mathrm{tar}}^{k+1} = U_{\mathrm{tar}}^{k} - U_e^* X \tag{18}$$

with

$$X = (U_e^{*T} U_e^*)^{-1} U_e^{*T} U_{\mathrm{tar}}^k \tag{19}$$

In Eq. (18) U_e^* is the best matching signature in iteration $k = 1$. The next step is to find the elemental signature which best matches the vector space of the new target space defined in Eq. (18). The signature identified in the previous iteration is not considered for matching in subsequent iterations. The entire process is repeated until the best matching elemental signature is near orthogonal to the target space. The result of this process is a set of elemental signatures which span the vector space of the original target vector space. The associated elemental stiffness matrices are considered strong possible locations of damage.

III. Evaluation of Reduced Models for Elemental Signature Recognition

Two important properties of reduced models raise issues in the subspace recognition algorithm. The first is that an elemental stiffness matrix may reside in the null space of the transformation matrix. That is, $K_e^j \in \mathrm{null}(T^T)$. This property is a result of the particular selected analysis set. Two implications arise. The first is that a stiffness perturbation in elements such as these will not induce a mode-force error in the reduced dynamic residual matrix in Eq. (9). The second implication is that calculation of the elemental signature with Eqs. (13) and (14) will be trivial. The second property is the possibility that two or more elements produce collinear signatures. Collinear residuals arise from two separate operations in the subspace recognition algorithm. The first operation is the reduction of the elemental stiffness matrix by Eq. (13). In certain cases, multiple reduced elemental stiffness matrices span identical space. This will guarantee collinear signatures regardless of the modal matrix postmultiplication. The second operation is postmultiplication of the reduced elemental stiffness matrix with the modal matrix in Eq. (14). Because the reduced stiffness elemental stiffness matrix is rank deficient, the possibility exists for collinear residuals to arise from the space transformation in the left-hand side of Eq. (14). The primary implication is that the elemental signature which best matches the target vector space can no longer be uniquely considered the sole location of damage if the signature has a collinear alias. In this case, one is forced to consider all other signatures in a collinear signature cluster as possible locations of damage. Before implementation of the subspace recognition algorithm, one must perform a pretest evaluation of the reduced model for null-signature elements and for collinear signatures. In addition, in the post-test, predamage assessment stage, one must also perform a survey for collinear signatures due to postmultiplication of the reduced elemental stiffness matrix with the modal matrix.

A. Transformation Matrix Null Space Test

Given a selection of an analysis set, the transformation matrix and the set of elemental stiffness matrices, the elemental stiffness matrices which fail the following criteria are considered members of $\mathrm{null}(T^T)$

$$|T^T K_e^j| < \propto \tag{20}$$

The elemental stiffness matrices that fail this criterion cannot be transformed into the reduced coordinates. For completeness, one may consider a range of tolerance values for identification of those elements which may produce a relatively small magnitude residual.

B. Collinear Signature Test

Frequently, due to structural symmetry and analysis-set location, multiple stiffness elements may produce similar eigenstructure sensitivities which are difficult or impossible to distinguish. In previous research, it has been shown that multiple perturbed stiffness elements can produce collinear mode shape sensitivities due to sensor location [14]. However, the issue regarding collinearity in this study is the collinearity of residuals produced by the combination of reduced elemental stiffness matrices and experimental modes. The sole basis of similar eigenstructure sensitivities alone will not guarantee that those stiffness elements will exclusively produce collinear signatures. The evaluation of reduced models for collinear signatures will be divided into two stages. In the pretest analysis, one must identify clusters of stiffness elements which produce collinear residuals as a result of having identical range in reduced coordinates. This will happen if multiple reduced elemental stiffness matrices can be rotated into each other. To determine if this is the case, the orthogonal procrustes problem is solved [13]. The formulation starts with

$$\Pi_{ij} = \min |\Gamma_i - \Gamma_j Q|_F \tag{21}$$

with

$$Q^T Q = I \tag{22}$$

$$\Gamma_i = T^T K_i^e T \tag{23}$$

$$\Gamma_j = T^T K_j^e T \tag{24}$$

$$i \neq j = 1, 2, 3, \ldots, n_e \tag{25}$$

where n_e is the number of candidate elements for $i, j = 1, 2, 3, \ldots,$. If there exists a matrix Q which forces Π_{ij} to zero, then $T^T K_i^e T$ and $T^T K_j^e T$ span identical space. Practically, the designation of collinearity should be established for a value of Eq. (21) to near machine zero. This also forces each column of the elemental signature found in Eq. (14) to be collinear given *any* set of experimental mode shapes. The optimal Q is found with the following SVD-based procedure:

$$C = \Gamma_i^T \Gamma_j \tag{26}$$

$$C = U \Sigma V^T \tag{27}$$

$$Q = U V^T \tag{28}$$

The matrix Q will minimize Eq. (21). The pretest analysis is therefore to analyze the set of elemental stiffness matrices for range similarity in the reduced coordinate system. All pairs of elemental stiffness matrices in reduced coordinates that result in a value near machine zero for Eq. (21) are considered collinear aliases of each other. The post-test, predamage assessment analysis is dependent on the measured modal matrix. Before, elemental stiffness matrices which span identical space in the reduced coordinate system were identified, and it was concluded that the signatures will also be collinear regardless of the projection onto the experimental modal matrix. However, when the reduced elemental stiffness matrices are projected onto the experimental modal matrix, the potential arises for additional elements to produce similar signatures on a mode-by-mode basis. To assess the similarity between the dynamic residual of two elemental stiffness matrices, the following modal assurance criterion (MAC) value is calculated

$$X_{ij}^p = \mathrm{MAC}(\Gamma_i \phi_p, \Gamma_j \phi_p) \tag{29}$$

where $\phi_p = p$th test mode. Two residual vectors are considered collinear when the MAC is greater than some specified tolerance near unity. The case may arise where stiffness elements produce collinear residual vectors for only a subset of the total residual vectors while other residuals may be distinguishable. Full spectrum collinearity is required for the resultant signatures to be indistinguishable. For instance, if stiffness elements 1 and 2 produce collinear residuals for modes 1, 2, 3, 4, but not 5, then elements 1 and 2 can be distinguished. However, if all five residuals are collinear, then elements 1 and 2 are indistinguishable. Collinear elemental signatures are a less severe limitation to damage localization than stiffness elements which reside in null(T^T). The limitation is that a signature which best matches the target vector space no longer uniquely implies its parent element as damaged. It also implies all other elements with collinear signatures as possible locations of damage.

IV. Example Structure 1: 155 mm Aeroshell

The 155 mm aeroshell is modeled in an FEM software package with an aluminum material and contains 864 shell elements and a total of 5328 global degrees of freedom. An analytical damage scenario is created by perturbing the modulus of elasticity of an unmeasured element. The aeroshell model, coarse and fine analysis sets of degrees of freedom and a damage location, E-65, are shown in Fig. 1.

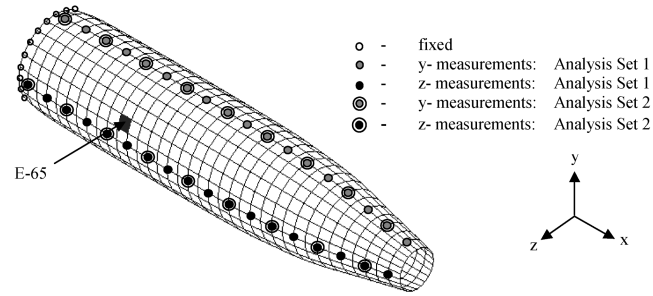

Fig. 1 155 mm cantilevered aeroshell.

In this case damage is defined as a 50% loss in elastic modulus for stiffness element 65. Only Guyan model reduction is considered in this example. There are two analysis sets of degrees of freedom shown in Fig. 1. The fine measurement set includes 72 radial measurements while the coarse set includes 36 radial measurements. The nominal reduced stiffness matrix was refined with MRPT using the first two flexible modes which were the first bending mode and the orthogonal first bending mode. In each of the two reduced models no elemental signatures produced collinear aliases in the pretest or predamage assessment stages. In addition, no elements in either reduced model resided in the null space of the transformation matrix. Each elemental signature was created on the basis of the first two flexible modes from the damaged structure of the same type as in the healthy refinement. The tolerance values for the selection of rank of elemental stiffness matrices were selected such that the target signature and each elemental signature were single column vectors. In addition, the algorithm was run until each elemental signature was assigned a principal angle rating. The results of the damage detection assessment for 864 iterations are presented in Figs. 2 and 3.

The algorithm was able to identify the correct damaged element in the first iteration with both analysis sets. Moreover, subsequent elemental signatures in analysis set 1 were localized near the damage area despite orthogonalization of the target signature with respect to the previously best matching signature. This arises from an imperfect removal of the damaged element signature from the original target signature due to the weakly nonlinear dependence on damage magnitude. The numeric values of the principal angle alignment of each damage detection study for the first 15 iterations are presented in Fig. 4. The first iteration identifies the best signature, rates its alignment to the target space, modifies the target, searches for the next best signature, and so on. The corresponding element number is shown atop each bar. The quantity in radians defined by θ_s where $s = 1$ of Eq. (17) is presented at each iteration.

The results of analysis set 1 strongly indicated the correct damage element number 65 in the first iteration. Subsequent elemental signatures rated closer and closer to an indication of orthogonality. In analysis set 2, the correct damaged element was identified in the first iteration. Notice that the rate of change with respect to the iteration of the principal angle alignment is a strong indicator of the convergence of the algorithm. For analysis set 1, it seems that significant signature matching is occurring after the first iteration. In analysis set 2, however, it appears that elemental signatures are modeling incoherent modeling errors and slight signature vector space deviations due to weak dependence on damage magnitude.

V. Example Structure 2: NASA Eight-Bay Truss

The eight-bay hybrid-scaled truss used in this investigation was part of the dynamic scale model technology program at NASA Langley Research Center [15]. Among other studies, a complete analytical and experimental analysis of this truss was performed providing a realistic test bed for structural damage localization/extent algorithms [16]. The truss configuration used in this example was cantilevered and instrumented with 96 accelerometers to measure all three translational degrees of freedom at each of the 32 unconstrained

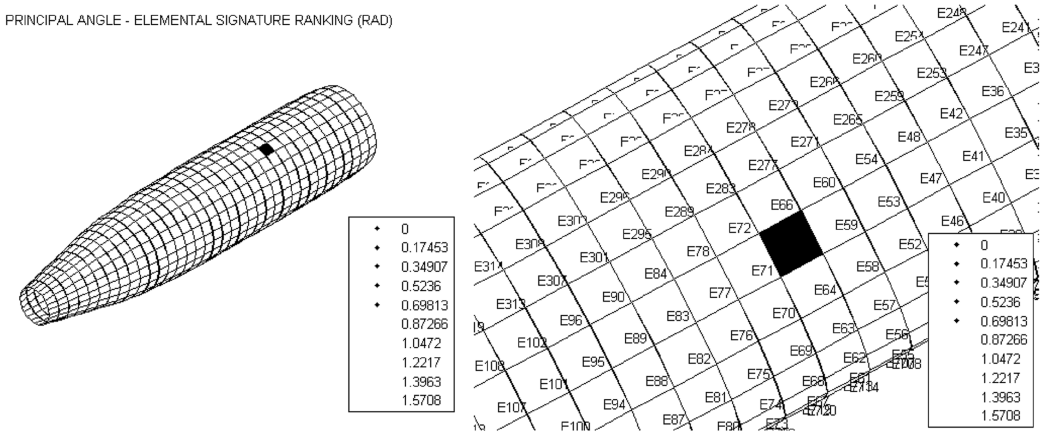

Fig. 2 155 mm cantilevered aeroshell. Elemental signature principal angle ranking for analysis set 1: 72 degrees of freedom; nominal model refinement: modes 1 and 2; damage detection: modes 1 and 2.

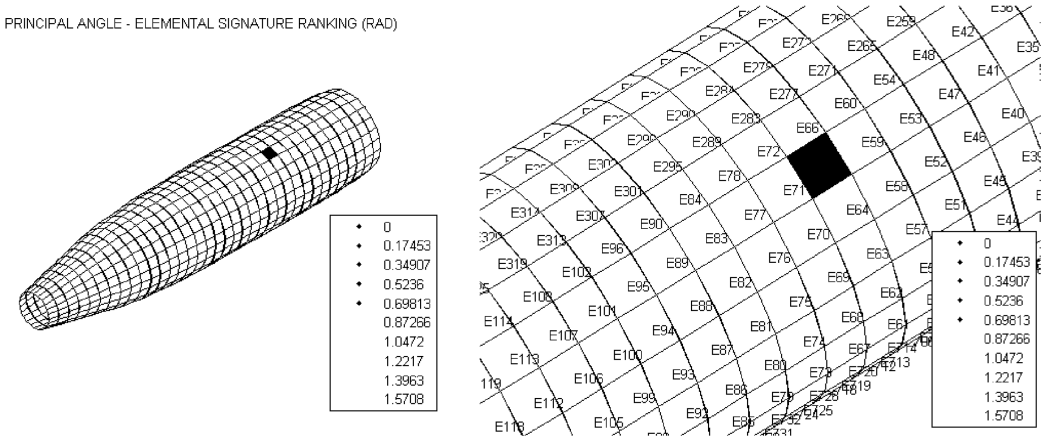

Fig. 3 155 mm cantilevered aeroshell. Elemental signature principal angle ranking for analysis set 2: 36 degrees of freedom; nominal model refinement: modes 1 and 2; damage detection: modes 1 and 2.

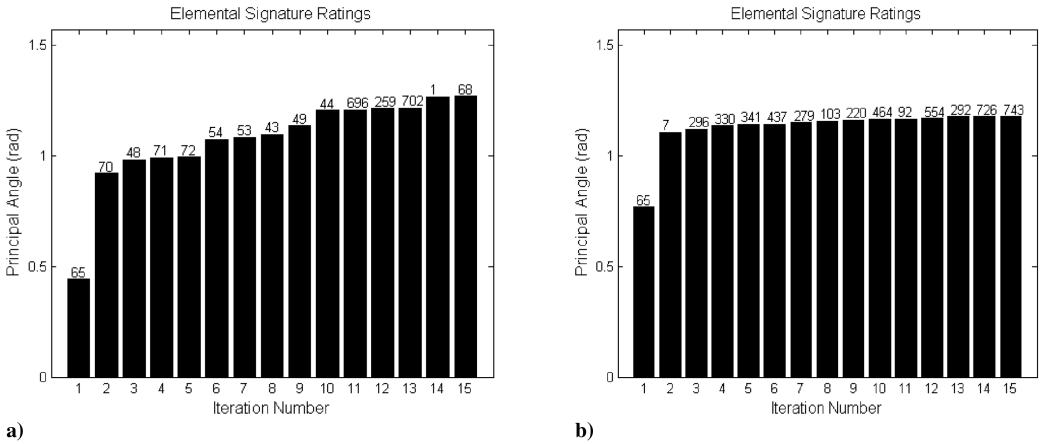

a) b)

Fig. 4 Damage case signature match: a) 72 degrees of freedom TAM; b) 36 degrees of freedom TAM.

nodes. A schematic of the truss is shown in Fig. 5 with different damage cases highlighted and a reduced sensor set shown. The first five global modes of vibration were identified in each modal survey. In all, 15 different damage situations were tested and experimental data were made available to researchers. In 13 cases, A, C–N, one truss member was removed. In case O, two struts, one longeron, and one diagonal were removed. In case P, one undamaged batten was replaced with a buckled strut. With the luxury of having all FEM degrees of freedom instrumented, any reduced set of measurements can be obtained by simply ignoring certain measurements. The instrumented nodes selected minimize the number of damage cases in which an affected degree of freedom was sensed.

A. Transformation Matrix Null Space Testing

The null space of the transformation matrix was tested for Guyan, IRS, and dynamic reduction. The minimum allowed value of μ in Eq. (20) was set at $1e$-10 and again at $1e$-5 and $1e$-3 for

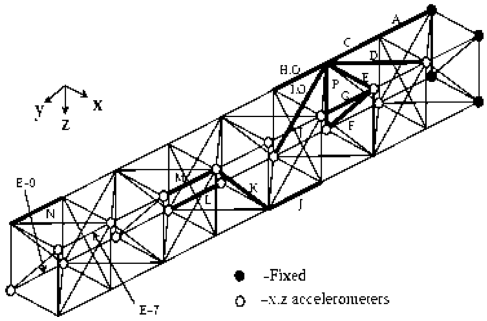

Fig. 5 NASA eight-bay damage cases and reduced sensor set.

completeness. For each value of μ the Guyan reduction method flagged elements 7 and 9 as being collinear aliases, whereas IRS and dynamic reduction methods did flag any elements as being collinear aliases. Elements 7 and 9 are indicated in Fig. 5. This indicates that stiffness elements 7 and 9 reside in the null space of the Guyan transformation matrix. The Guyan reduction method cannot reduce these elemental stiffness matrices and as a consequence, damage in these elements cannot be detected. However, the IRS and dynamic reduction methods for all test modes can sense damage in these elements.

B. Collinear Signature Testing

The pretest analysis developed in Sec. III was performed using the IRS and Guyan reduction methods. Only Guyan reduction produced reduced elemental stiffness matrices with identical range according to Eq. (21). It is not possible to know a priori any of the dynamic transformation matrices if the transformation is based on the damaged experimental natural frequency. The graph in Fig. 6 shows all pairs of stiffness elements with identical range in reduced coordinates. Each grid line corresponds to a stiffness element while an asterisk marks a pair of elemental stiffness elements that have identical range in reduced coordinates. These pairs of elemental signatures minimized Eq. (21) to near machine zero. Before we construct a single mode-dependent elemental signature, we know that pairs of signatures indicated above are guaranteed to produce collinear signatures when using Guyan reduction.

The post-test, predamage assessment analysis was performed with modal data from cases O and J. Collinear residuals were identified using Eq. (29) with a cutoff MAC of 0.90. These pairs produced collinear residuals for all five test modes as shown in Fig. 7. The predamage assessment for the Guyan reduced model revealed no additional collinear residuals beyond those identified in the pretest study.

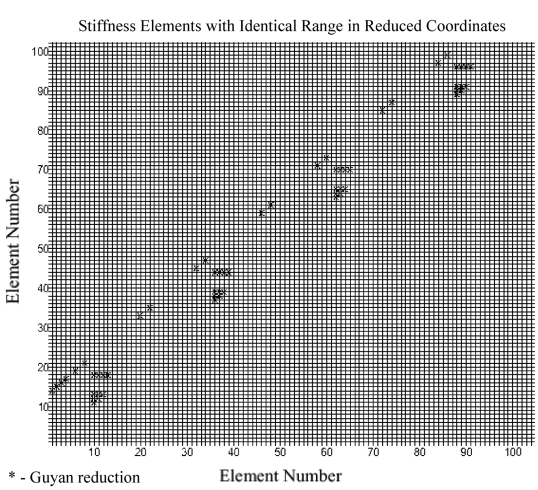

Fig. 6 Pretest screening for collinear signatures.

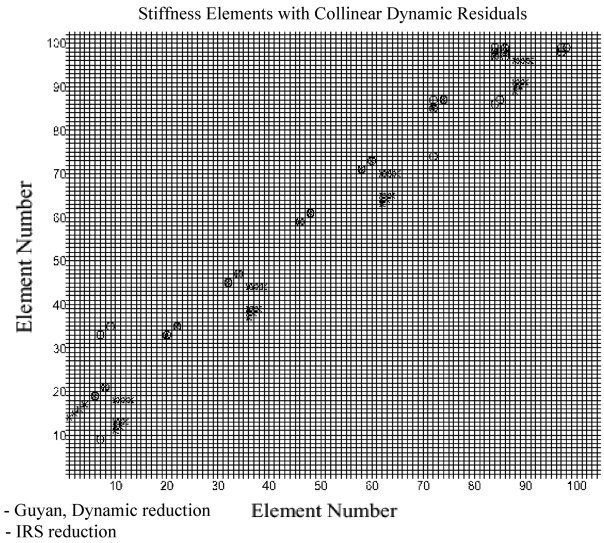

Fig. 7 Post-test, predamage assessment screening of collinear signatures.

Stiffness elements 7 and 9 were excluded from this survey because no reduced coordinate information could be produced with Guyan reduction. Dynamic reduction created pairs of collinear residuals exactly the same as those given by Guyan reduction. The IRS method caused stiffness elements to produce collinear residuals that were not predicted in the pretest analysis by the Guyan model reduction study.

C. Informed Damage Detection Results

The signature recognition algorithm was executed on damage cases O and J. The results are shown in Figs. 8 and 9 for 15 iterations and three reduction methods. Case O is the two-member damage case in which element nos. 81 and 73 were removed. Case J involved the removal of member no. 58. As the matching of the target vector space becomes complete, the principal angle rating indicates an orthogonal alignment of the target and elemental signature. The damaged elements are identified when the signature rating approaches orthogonality to some constant.

A first look at the results of case O seems to indicate a split decision on the location of damage. That is, the Guyan-based method indicated elements 73 and 81 to be damaged, whereas IRS indicated 81. The dynamic-based method indicated elements 60 and 81 as damaged. However, investigation of the collinear pairs in Figs. 6 and 7 indicate that elements 60 and 73 are collinear aliases of each other for Guyan and dynamic reduction. We can now be confident that the three approaches are not split in damage localization but that the vector space of perturbed stiffness element 81 and the common vector spaces of perturbed elements 60 and 73 are strongly represented in the target vector space. When two elements have collinear aliases, in theory they have equal principal angles. However, due to measurement noise and computation resolution, they will always be slightly different. In the case of using dynamic reduction, element 60 had a slightly larger numerical value than element 73 and was thus chosen. With the space spanned by element 71 (or 60) removed from the target vector, the remaining space is used to identify element 81. So essentially there are two candidates for damage as indicated by the Guyan- and dynamic-based methods. The informed damage localization result identified the correct two damaged members for case O. This example shows the importance of performing the initial collinearity study.

In case J, all three reduction methods strongly indicated a collinear alias of the true damaged element. The collinear alias for all three reduction methods for stiffness element 71 is the true damaged element 58. This conclusion cannot be made without a study of signature collinearity for this model. The fact that stiffness elements 7 and 9 could not be reduced with Guyan reduction did not hinder the performance of the algorithm in these cases.

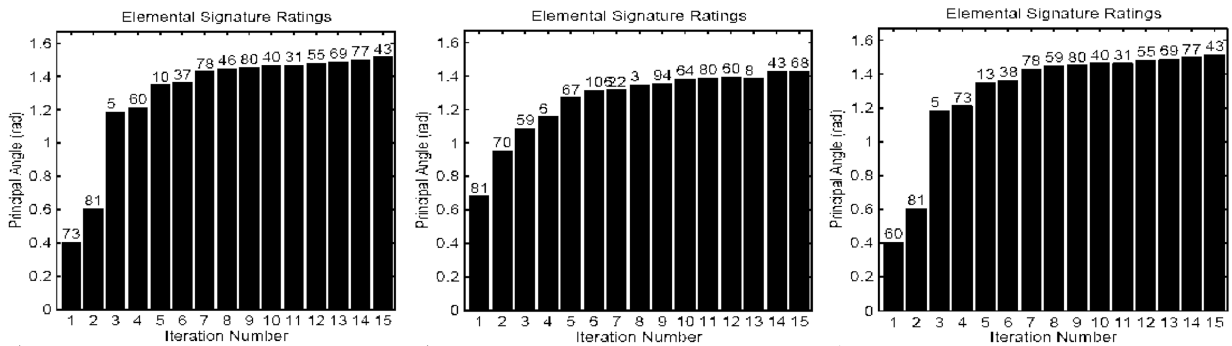

a) b) c)

Fig. 8 Case O signature match: a) Guyan reduction; b) IRS reduction; c) dynamic reduction.

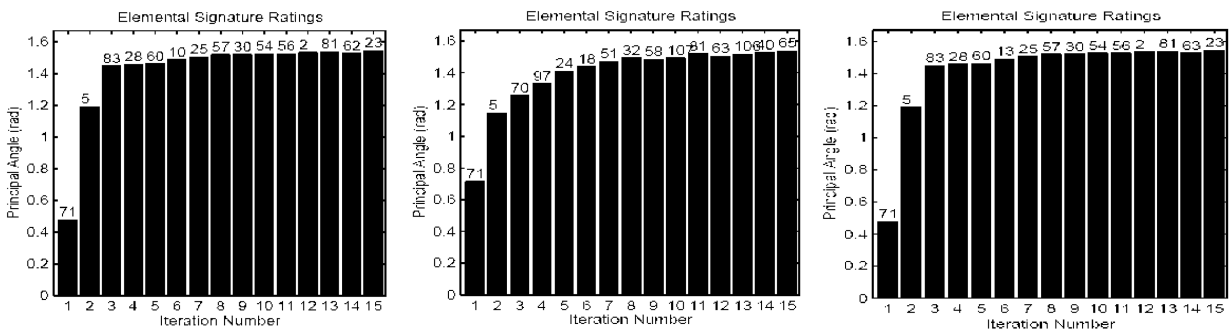

a) b) c)

Fig. 9 Case J signature match: a) Guyan reduction; b) IRS reduction; c) dynamic reduction.

VI. Summary and Conclusions

A method for damage localization using subspace recognition with incomplete modal measurements was presented. The characteristic mode-force error in the reduced dynamic residual resulting from the corruption of load path information was regarded as a signature of a stiffness element. It was observed that two aspects of reduced models must be accounted for in the algorithm. First is the inability of certain transformation matrices to project elemental stiffness matrices in the reduced coordinates, and the second is the nonuniqueness of reduced dynamic residuals. Methods for evaluating these two aspects of reduced models were proposed to assess their suitability for damage localization using subspace recognition. A simple transformation matrix null space test was developed to identify elemental stiffness matrices that cannot be reduced to the analysis set of coordinates. Two reduced dynamic residual collinearity tests were developed. The first test identified collinear residuals by finding elemental stiffness matrices with identical range in the reduced coordinates. Evaluation of a reduced model before the onset of modal testing will provide a reasonable assessment of identifiable stiffness elements. The second test found collinear residuals by an exhaustive comparison between generated residuals using the modal assurance criterion. The elements identified in the second test were shown to identify stiffness elements not identified in the first test.

The elemental signature recognition procedure was applied to a 155 mm aeroshell and two experimental damage cases of the NASA eight-bay model using three model reduction methods (Guyan, improved reduced system, and dynamic). The 155 mm aeroshell study included a fine and a coarse reduced measurement set for damage assessment. In either case, no collinear elements were identified at any stage of the damage assessment and no elemental stiffness matrices produced null signatures. The aeroshell model included over 5 K degrees of freedom and was able to localize damage using a minimum of 36 degrees of freedom in the test analysis model based on the Guyan model reduction technique. The damage detection effort was based on assuming that only two flexible modes of vibration are measured in the healthy and damaged states. In the reduced model assessment of the NASA eight-bay structure, it was found two elemental stiffness matrices resided in the null space of the Guyan transformation matrix. Therefore, perturbation in the stiffness of these two elements would not produce a residual force imbalance in reduced coordinates, making damage localization for these elements impossible. It was also determined that multiple clusters of elemental signatures were collinear. There existed different sets of collinear signatures depending on the model reduction method used. The results of the damage localization algorithm based on three reduction methods appeared to give split results in the first damage case and erroneous results in the second. It was found, upon referencing identified collinear signatures, that the split case was indeed indicating two different elements with collinear signatures in reduced coordinates. The conclusion was that there was not a split indication of the elemental signature present in the damaged experimental data. The second case study simply indicated a collinear alias of the true damaged element. These studies support the conclusion that the performance of the subspace recognition approach for damage localization can correctly identify the correct damaged elements or, if any, the associated collinear. This ability, however, is dependent on the damage level and the coherency of the residual vector space within measurement capabilities of the selected sensor set. When damage is isolated to a member that does have a collinear alias, damage can only be narrowed down to the member and the family of collinear aliases. Indeed, the assumption of damage being accurately represented by a localized perturbation to a stiffness matrix model is valid for a large class of damage scenarios but is not an exhaustive approach.

Acknowledgments

The authors wish to acknowledge the National Science Foundation, Grant No. CMS0116193. The second author also wishes to acknowledge the support of the Texas Institute for Intelligent Bio-Nano Materials and Structures for Aerospace Vehicles, funded by NASA Cooperative Agreement No. NCC-1-02038.

References

[1] Mottershead, J. E., and Friswell, M. I., "Model Updating in Structural Dynamics—A Survey," *Journal of Sound and Vibration*, Vol. 30, No. 2, 1993, pp. 347–375.

[2] Doebling, S. W., Farrar, C. R., and Prime, M. B., "A Summary Review of Vibration-Based Damage Identification Methods," *The Shock and Vibration Digest*, Vol. 30, No. 2, 1998, pp. 91–105.

[3] Zimmerman, D. C., and Smith, S. W., "Model Refinement and Damage Location For Intelligent Structures," *Intelligent Structural Systems*, Kluwer, Norwell, MA, 1992, pp. 403–452.

[4] Baruch, M., and Bar Itzhack, I. Y., "Optimum Weighted Orthogonalization of Measured Modes," *AIAA Journal*, Vol. 16, No. 4, 1978, pp. 346–351.

[5] Martinez, D., Red-Horse, J., and Allen, J., "System Identification Methods for Dynamic Structural Models of Electronic Packages," *Proceedings of the Thirty Second Structural Dynamics and Materials Conference*, AIAA, Washington, D.C., 1991, pp. 2336–2346.

[6] Matzen, V. C., "Time Domain Identification of Reduced Parameter Models," *Proceedings of the Society for Experimental Mechanics Spring Conference on Experimental Mechanics*, Society for Experimental Mechanics, Bethel, CT, 1987, pp. 401–408.

[7] Zimmerman, D. C., and Widengren, W., "Model Correction Using a Symmetric Eigenstructure Assignment Technique," *AIAA Journal*, Vol. 28, No. 9, 1990, pp. 1670–1676.

[8] Kaouk, M., and Zimmerman, D. C., "Structural Damage Assessment Using a Generalized Minimum Rank Perturbation Theory," *AIAA Journal*, Vol. 32, No. 4, 1992, pp. 836–842.

[9] Zimmerman, D. C., Kim. H. M., Bartkowicz, T. J., and Kaouk, M., "Damage Detection Using Expanded Dynamic Residuals," *Journal of Dynamic Systems, Measurement, and Control*, Vol. 123, No. 4, 2001, pp. 699–705.

[10] Lopez, F. P., and Zimmerman, D. C., "A Pattern Recognition Approach for Damage Localization Using Incomplete Measurements," *Proceedings of the Seventeenth International Modal Analysis Conference*, Society for Experimental Mechanics, Bethel, CT, 1999, pp. 579–585.

[11] James, G., Zimmerman, D. C., and Cao, T., "Development of a Coupled Approach for Structural Damage Detection," *Proceedings of the Thirty-Fifth Aerospace Sciences Meeting and Exhibit*, AIAA, Washington D.C., Jan. 1997; also AIAA Paper 97-0362.

[12] Zimmerman, D. C., and Simmermacher, T., "Model Correlation Using Multiple Static Load and Vibration Tests," *AIAA Journal*, Vol. 33, No. 11, 1995, pp. 2182–2188.

[13] Golub, G. H., and Van Loan, C. F., *Matrix Computations*, Johns Hopkins Univ. Press, Baltimore, MD, 1996, pp. 603–604.

[14] Cobb, R. G., and Liebst, B. S., "Sensor Placement and Structural Damage Identification from Minimal Sensor Information," *AIAA Journal*, Vol. 35, No. 2, 1997, pp. 369–374.

[15] Kashangaki, T. A. L., "Ground Vibration Tests of a High Fidelity Truss for Verification of On Orbit Damage Location Techniques," NASA LaRC 107626, 1992.

[16] Zimmerman, D.C., Smith, S. W., Kim, H.-M., and Bartkowicz, T., "An Experimental Study Of Structural Damage Detection Using Incomplete Measurements," *Journal of Vibration and Acoustics*, Vol. 118, No. 4, 1996, pp. 543–550.

C. Pierre
Associate Editor